Signal Processing and Renewable Energy
December 2020, (pp. 39-52)
ISSN: 2588-7327
eISSN: 2588-7335

Parameters Estimation of the Inverter Connected to a Single-Phase Full-Bridge Photovoltaic System with Adaptive Chaotic Grey Wolf Algorithm to Synchronize Phase and Frequency

Ali Akbar Farjami [1], Mahdi Yaghoobi [1*]

[1] Electrical Engineering Dep., Mashhad Branch, Islamic Azad University, Mashhad, Iran.

Received: 20-Mar-2020, Revised: 26-May-2019, Accepted: 04-Sep-2020.

Abstract
Photovoltaic (PV) systems are widely used due to low maintenance costs and being non-pollutant. Selecting proper parameters for the inverter is essential for its stable performance. The inverter connected to the grid should be able to transfer maximum PV energy to the power grid. To have the complete transmission, the output current of the inverter should be synchronous with the voltage of the power network in terms of phase and frequency. The inverter affects the quality of the power generated by the PV and chaotic behavior can affect the performance of the PV system, negatively. Due to chaotic behavior, by determining the correlation coefficient, PV voltage and circuit parameters, phase and frequency can be synchronized. Therefore, in this paper, determining parameters of the inverter connected to the single-phase full-bridge PV system for phase and frequency synchronization is studied. To increase the accuracy of estimating system parameters and reduce synchronization error, the adaptive chaotic grey wolf Algorithm is used. Simulations are compared with PSO and GWO indicating the superiority of the proposed method in terms of phase and frequency synchronization.

Keywords: Parameter Estimation; Synchronization; Full-bridge Photovoltaic; Grey Wolf Algorithm.

1. INTRODUCTION

Solar energy as one of the renewable energy resources has attracted significant attention in recent years due to its positive environmental effects and being non-pollutant [1]. This energy is converted to electrical energy via PV arrays. Recently, PV generation has attracted attention because of its being non-pollutant and not consuming fuel [2]. The grid-connected inverter is used to connect each PV system to the grid [3]. Grid-connected PV systems are widely used in

*****Corresponding Authors Email: yaghoobi@mshdiau.ac.ir

various applications [4-6]. The grid-connected inverter plays an important role in connecting the PV system to the power grid. Therefore, its behavior impact on the PV generation system is very important [7,8]. Nonlinear behavior particularly chaotic behavior occurs in power electronic systems [9-12]. In [9], PID controller has been used to obtain the input voltage of the Cuk converter such that it shows no chaotic behavior and it is set to a specific value. In [10], the stability of a boost converter supplied with a PV source has been studied. In [11], nonlinear dynamics and bifurcation of a boost converter for charging the battery in PV applications have been studied. In [12], the dynamic behavior of a full bridge DC-AC inverter has been studied using constant frequency pulse width modulation and it is shown that by changing control parameters and input voltage, fast and slow instabilities occur in the system.

Since the accuracy of the structure and values of the key parameters affect the simulation results directly, parameter identification has great importance [13]. Unknown parameters in grid-connected PV systems are mainly related to the inverter and the PV array. Till now, various studies have been done to optimize the parameters of the PV array [13-19]. In [20-22], typical numerical methods have been used to identify parameters of the PV inverter. Without considering internal shape of the inverter and the logical system controller relationship, the inverter is equivalent to a multiple-input multiple-output system.

In some studies, the issue of identification and control in inverters in micro grids has been considered. In [23], the design of an interconnected converter control system based on the identification of a DC sub-grid model system was presented in a hybrid AC / DC micro grid. In [24], the application of a precision-based aggregation technique for the analysis of large-scale networks with control drop inverters was presented.

In [25], simultaneous identification of several control loops in dc micro grid power converters was proposed by injecting a quasi-randomized binary sequence and measuring the loop yield of a loop in a cycle. In [26], linear programming of the correct mixture number presented to identify the distribution network using inverter exploration.

In [27], the stability characteristics of micro grid-based inverters were examined by identifying the possible presence of groups of inverters called critical clusters along with their control settings to approach the stability range. In [28], DC-DC buck converter identification was performed using the relay feedback method with experimental validation.

In [29], advances were made on system identification techniques for switching power switches. In [30], the estimation of DC-DC converter parameters was studied using regression algorithms with adjustable iteration frequency. In [31], the controller parameter was identified for the photovoltaic inverter based on the minimized squared method. A comparison between the model parameters and the identified parameters of the inverter showed the flexibility and accuracy of the proposed method. In [32] the modeling of the photovoltaic network connected to the generation system based on the parametric identification method was presented. To obtain the photovoltaic model with precise parameters, the least squares recursive method and the measured photovoltaic and photovoltaic inverter data were used to develop the identification of the network-connected photovoltaic system. In some studies, meta-heuristic optimization algorithms have been used to identify inverter parameters.

In [33], a two-step method for identifying network-connected inverter control parameters was proposed based on the differential evolution algorithm. In [34], the identification of the network-connected inverter model parameter was proposed using the particle swarm optimization algorithm combined with the simulated annealing. The results showed that this proposed method performed better in terms of high accuracy and convergence speed compared to other similar optimization algorithms. Table 1 summarizes the sources associated with identifying inverter parameters.

In [1], the inverter connected to the single-phase full-bridge PV system has been introduced. Analyses have shown that the system represents chaotic behavior under particular conditions. Therefore, a unidirectional correlation method has been proposed for synchronization which is simpler than similar schemes. In addition, system parameters are assumed to be known. In practical applications, system parameters might not be available. Furthermore, proper selection of parameters affects the stable performance of the system. Therefore, parameters can be determined such that phase and frequency are synchronized with higher accuracy.

TABLE 1. ***Sources associated with identifying inverter parameters.***

Authors	Title	Description
Tang et al [1]	Synchronization control of single-phase full bridge photovoltaic grid-connected inverter	In this paper, phase synchronization and inverter frequency connected to the photovoltaic network were performed. But the parameters were clear.
Chang et al [31]	Parameter Identification of Controller for Photovoltaic Inverter Based on L-M Method	The unknown parameters of the power electron converter controller are estimated based on the dampened least squares. This article uses a linear model.
Jiayu et al [32]	Modeling of photovoltaic grid connected generation system based on parameter identification method	Key parameters of the PV model were found. The least squares recursive method was used to develop the identification of the network-connected PV system parameter. The problem with this approach is that it may be trapped in local optimal.
Liu et al [33]	Two-step method for identifying photovoltaic grid-connected inverter controller parameters based on the adaptive differential evolution algorithm	The adaptive differential evolution algorithm was used to estimate the inverter model parameters. This paper does not discuss the phase synchronization and frequency of inverter behavior.
Xu and Jin [34]	A parameter identification model for the Photovoltaic grid-connected inverter	The control parameters are identified by analyzing the PV double inverter open loop control system. The particle optimization algorithm combined with the simulated recycling algorithm was used to identify controller parameters. In this paper, there is no discussion about chaotic behavior and phase and frequency synchronization of the inverter.

Considering the previous studies, determining parameters of the inverter for synchronizing phase and frequency has not been studied. In this paper, PV-connected inverter parameters are determined to synchronize phase and frequency. To this end, an adaptive chaotic grey wolf optimization algorithm is presented. The algorithm's global ability has been improved with the aid of Chebyshev's chaotic mapping. Also, the parameter ‘a’ is adapted and the balance is established between the local and global search of the algorithm.

In this scheme, circuit parameters and unidirectional correlation coefficient and PV voltage are determined such that the output current of the inverter is synchronized with the grid voltage in terms of phase and frequency.

The structure of this paper is as follows. Section 2 presents equations of the single phase full bridge PV grid-connected inverter. Section 3 formulates the problem. The proposed adaptive chaotic grey wolf algorithm is introduced in section 4. Section 5 presents the simulation results. Finally, the paper is concluded in section 6.

2. THE INVERTER CONNECTED TO THE SINGLE-PHASE FULL-BRIDGE PV SYSTEM

In [1], the inverter connected to the single-phase PV system is shown in Figure 1 and its equations are given. The main circuit includes DC/DC converter, DC/AC converter, filter and the controller circuit. According to Figure 1, the system model is as follows:

$$\begin{cases} \dot{i}_{L1} = -\dfrac{u_{C_0}}{L_1} + \dfrac{U_{pv}}{L_1} S_1 \\ \dot{u}_{C_0} = \dfrac{i_{L_1}}{C_0} - \dfrac{u_{C_0}}{C_0(R_1+R_2)} \\ \qquad - \dfrac{2S-1}{C_0}\left[(1-\eta_1)i_L + \eta_1 U_{ac}\right] \\ \dot{u}_i = \dfrac{R_2}{C_0(R_1+R_2)} i_{L_1} + \mu u_{C_0} \\ \qquad - \dfrac{R_2(2S-1)}{C_0(R_1+R_2)} i_L - \dfrac{u_i}{C_3 R_3} \\ \dot{i}_L = -\dfrac{1}{L} u_c + \dfrac{(2S-1)}{L} u_{C_0} \\ \dot{u}_C = \dfrac{1}{C} i_L - \alpha u_C + \beta u_{ac} \\ \dot{u}_{con} = -\dfrac{k}{C} i_L + \eta u_C + \delta u_{ac} + \gamma \omega v \\ \dot{u}_{ac} = \omega v \\ \dot{v} = -\omega u_{ac} \end{cases} \tag{1}$$

In the above equations, U_{pv} and η_1 are the PV voltage and the correlation coefficient. i_{L1}, u_{C0} and u_i are the inductor current, the capacitor voltage and control voltage of the DC/DC converter. i_L, u_C and u_{con} are the inductor current (output current of the inverter), the capacitor voltage and control voltage of the DC/AC converter. u_{ac} is the grid voltage.

In [1], all parameters of the system are assumed to be known. In this paper, all parameters of $\eta_1, U_{pv}, L_1, C_0, C_3, R_1, R_2, R_3, R_4$ are unknown and should be determined such that the phase and frequency of the output current of the inverter and the grid voltage are synchronized.

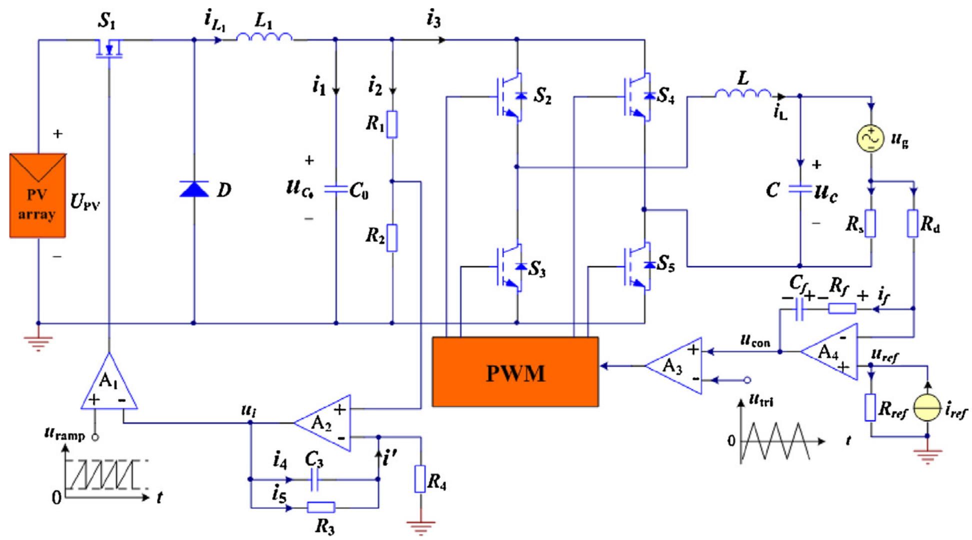

Fig. 1. The inverter connected to the single-phase full-bridge PV system.

3. PROBLEM FORMULATION

A nonlinear system can be formulated as follows:

$$\dot{X} = F(X, X_0, \theta) \tag{2}$$

For a single-phase inverter connected to PV system $X = (i_{L1},\ u_{C0},\ u_i,\ i_L,\ u_C,\ u_{con},\ u_{ac},\ v)^T$. X_0 is the initial condition of the system. In the above equation, θ is the vector of parameters written as in Eq. (3).

$$\theta = (\eta_1,\ U_{pv},\ L_1,\ C_0,\ C_3,\ R_1,\ R_2,\ R_3,\ R_4)^T \tag{3}$$

In this paper, system parameters are determined such that phase and frequency are synchronized. Accordingly, the proposed cost function includes frequency synchronization error and phase synchronization error as in Eq. (4).

$$\begin{aligned} Z_1 &= \frac{1}{N - T_1 - 1} \sum_{j=1}^{N-T_1-1} ((iL(j) - iL(j+T))^2) \\ Z_2 &= | u_{ac}(s_1) - iL(s_1) | \quad s_1 = \arg(\max(u_{ac})) \\ Z &= Z_1 + Z_2 \end{aligned} \tag{4}$$

Since frequency of the grid is 50Hz, in Eq. (4), $T_1 = \frac{1}{50dt}$. s_1 is the argument of maximum u_{ac}. In this function, Z_1 is associated with frequency synchronization in which i_L is repeated in a period similar to u_{ac}. Z_2 is associated to phase synchronization in which the phase between i_L and u_{ac} is similar and the two signals are aligned. Therefore, the maximum value of the two signals should be aligned as applied in Z_2. This cost function is calculated simultaneously in each evaluation. In the proposed scheme, unknown parameters are obtained using the adaptive chaotic grey wolf algorithm such that the cost function (4) is minimized.

4. THE ADAPTIVE CHAOTIC GREY WOLF ALGORITHM

In this paper, an adaptive chaotic grey wolf algorithm is used to determine parameters of the inverter connected to the PV system to synchronize phase and frequency. GWO is an intelligent optimization method inspired by social hunting behavior of the grey wolves.

The convergence rate of this algorithm is good and it is able to resolve being trapped in local optimums [35]. In this algorithm, 4 types of wolves, namely, alpha, beta, delta and omega are used to simulate the leadership hierarchy and three main steps of hunting including searching for the prey; encircling the prey and attacking the prey are executed.

The following equation is used to model the encircling procedure.

$$\vec{D} = \left|\vec{C}.\vec{X}_p(t) - \vec{X}(t)\right| \qquad \vec{X}(t+1) = \vec{X}_p(t) - \vec{A}.\vec{D} \tag{5}$$

In the mentioned equations, t is the iteration number, $\vec{A}$ and $\vec{C}$ are the coefficient vector, $\vec{X_p}$ is the prey position vector and $\vec{X}$ is the position vector of a grey wolf. Vectors $\vec{A}$ and $\vec{C}$ are calculated as follows:

$$\vec{A} = 2\vec{a}.\vec{r}_1 - \vec{a} \qquad \vec{C} = 2\vec{r}_2 \tag{6}$$

In which, components of $\vec{a}$ decrease from 2 to 0 linearly in subsequent iterations; $\vec{r}_1$ and $\vec{r}_2$ are random vectors in the range of [0,1].

Hunting procedure is modelled as in the following equations:

$$\vec{D}_\alpha = \left|\vec{C}_1.\vec{X}_\alpha - \vec{X}\right|, \quad \vec{D}_\beta = \left|\vec{C}_2.\vec{X}_\beta - \vec{X}\right|, \quad \vec{D}_\delta = \left|\vec{C}_3.\vec{X}_\delta - \vec{X}\right| \tag{7}$$

$$\vec{X}_1 = \vec{X}_\alpha - \vec{A}_1.(\vec{D}_\alpha), \quad \vec{X}_2 = \vec{X}_\beta - \vec{A}_2.(\vec{D}_\beta), \quad \vec{X}_3 = \vec{X}_\delta - \vec{A}_3.(\vec{D}_\delta) \tag{8}$$

$$\vec{X}(t+1) = \frac{\vec{X}_1 + \vec{X}_2 + \vec{X}_3}{3} \tag{9}$$

As complexity of the optimization problems increases, convergence rate of this algorithm decreases and consequently increases computation time. To solve this problem, new developments of this algorithm have been presented in various studies [36-38].

Using chaotic mapping improves algorithm convergence. In this article, Chabishev's chaotic mapping is considered, the relationship of which is as follows.

$$x_{k+1} = \cos(k \cos^{-1}(x_k)) \tag{10}$$

In this paper, an improved grey wolf optimization algorithm is introduced. In the presented algorithm, parameter a is updates as a nonlinear decreasing equation using Eq. (10) in each iteration as follows:

$$a(it) = \left(\frac{(MaxIt - it)}{(MaxIt - 1)}\right)^E (a_{\max} - a_{\min}) + 0.15z(it) \tag{11}$$

where z is chaotic mapping and E is the power and smaller than 1. a_{max} and a_{min} are the maximum and minimum values of 'a', respectively. To update position of the wolves, the following equations are used. If a random number larger than 0.5, Eq. (12) is used and if a random number larger than 0.1, Eq. (13) is used; otherwise, Eq. (14) is used.

$$X(t+1) = 0.4X1 + 0.35X2 + 0.25X3 + 0.01a*randn*(VarMax - VarMin) \tag{12}$$

$$X(t+1) = (X1 + X2 + X3)/3 + 0.05a * randn * (VarMax - VarMin) \quad (13)$$

$$X(t+1) = X(t) + 0.1a * randn * (VarMax - VarMin) \quad (14)$$

General flowchart of determining parameters of the inverter connected to the single-phase full-bridge PV grid using the adaptive chaotic gray wolf algorithm for synchronizing phase and frequency is shown in Figure 2.

5. SIMULATION AND RESULTS

To minimize the cost function, grey wolf optimization (GWO), particle swarm optimization (PSO) and adaptive chaotic grey wolf optimization (ACGWO) are used. The parameters of this algorithm are adjusted as follows. The population size is 40 and the maximum number of iterations is 60. Table 2 represents the results of executing the mentioned algorithms.

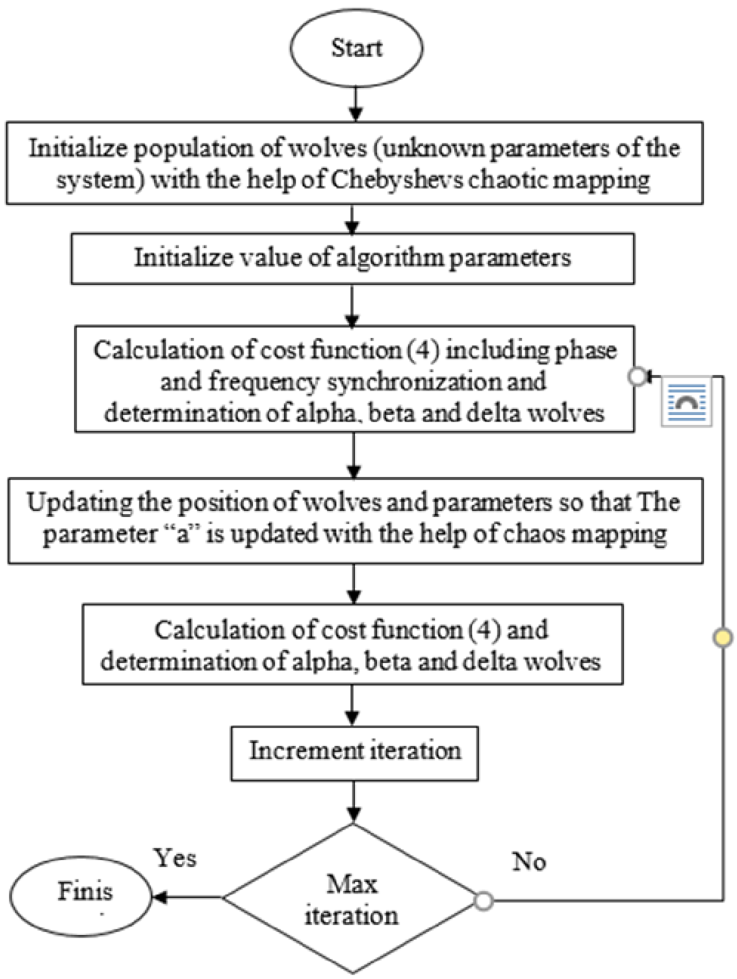

Fig. 2. Flowchart of determining parameters of the inverter using ACGWO for phase and frequency synchronization.

Table 2. ***Values of the parameters determined using GWO, PSO and ACGWO.***

Parameter	Range	Determined Value		
		GWO	PSO	ACGWO
η_1	[-3 -0.5]	-2.90836	-2.71858	-2.92795
U_{pv}	[10 60]	20.1086	21.8778	20.1499
L_1 (mH)	[50 250]	233.575	244.1192	227.6222
C_0 (μF)	[80 500]	241.4846	229.7597	246.0703
C_3 (nF)	[15 25]	23.3012	17.9341	18.2301
R_1 (Ω)	[40 400]	379.5645	399.6973	399.9888
R_2 (Ω)	[0.2 20]	1.8139	11.5330	18.638
R_3 (Ω)	[7000 15000]	12848	13004	11716
R_4 (Ω)	[500 1500]	1402.5	1242.3	1008.1

Table 3. ***Values of elements and total value of the cost function using GWO, PSO and ACGWO.***

Cost Function	GWO	PSO	ACGWO
Z_1 (Frequency synchronization)	12.1122	11.5277	10.6163
Z_2 (Phase synchronization)	1.3101	5.3457	0.1357
Z	13.4223	16.8743	10.752

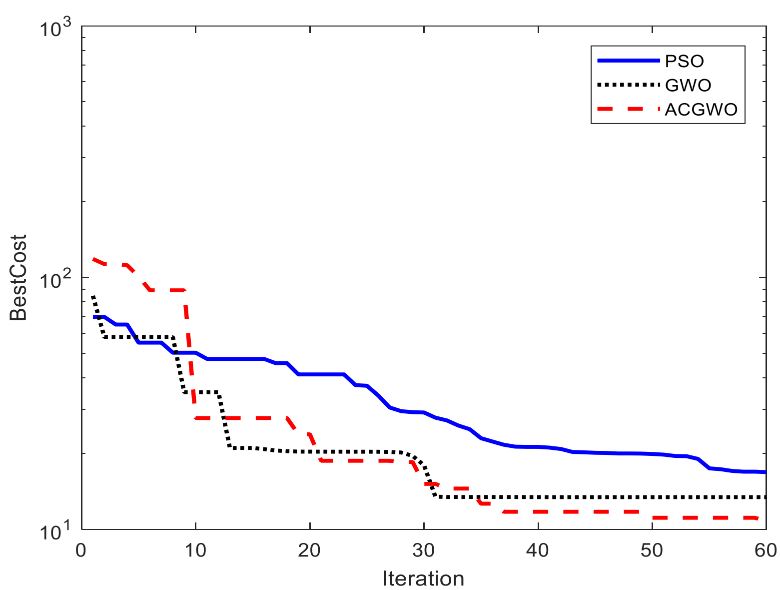

Fig. 3. Best cost vs. number of iterations.

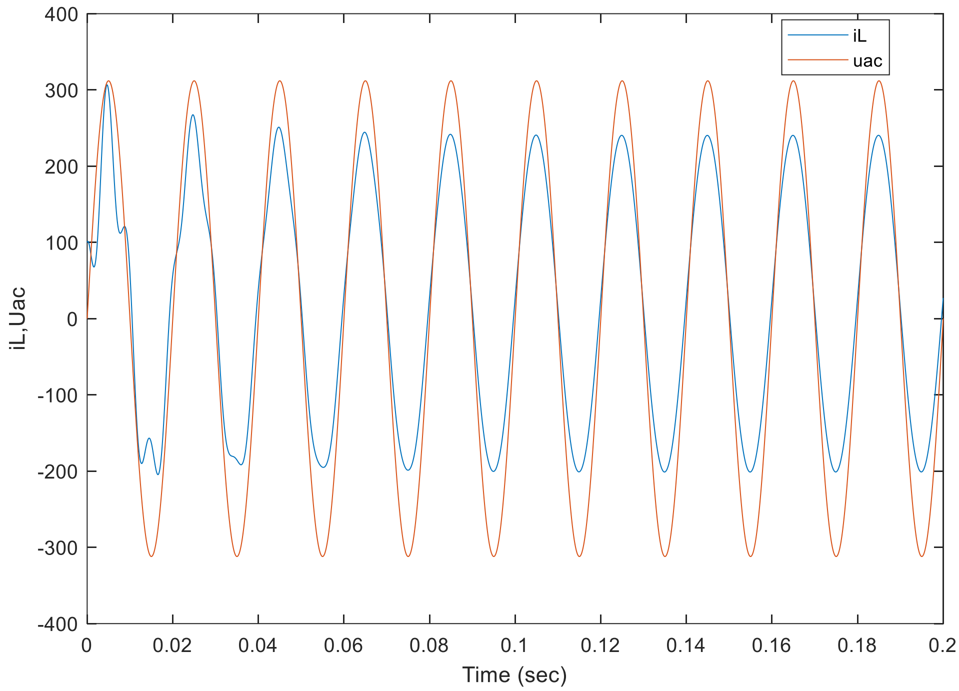

Fig. 4. The values of i_L and u_{ac} obtained using ACGWO.

Table 2 shows that the parameters might take different values for phase and frequency synchronization. Table 3 shows values of the elements of the cost function and total value of the cost function.

Table 3 shows that the ACGWO outperforms GWO and PSO in terms of best cost function. Curve of best cost function vs. number of iterations is shown in Figure 3. It can be seen in Figure 3 that from the 20^{th} iteration, ACGWO outperforms the other two algorithms in terms of accuracy. In addition, the proposed algorithm has obtained minimum cost function in fewer iterations.

Figure 4 shows output current of the inverter and the grid voltage obtained using ACGWO.

It can be seen in Figure 4 that after 0.05s, phase and frequency are synchronized. Figure 5 shows i_L and u_{ac} obtained from GWO, PSO and ACGWO.

According to Figure 5(b), the red curve is close to u_{ac} in terms of frequency synchronization compared to the blue and black curves. Furthermore, ACGWO has obtained better results in terms of phase synchronization compared to the other two algorithms. Therefore, the results show the efficiency of the proposed method in achieving phase and frequency synchronization.

6. CONCLUSION

In this paper, determining parameters for phase and frequency synchronization of an inverter connected to a single-phase full-bridge PV grid is presented. To solve this problem, a cost function including two

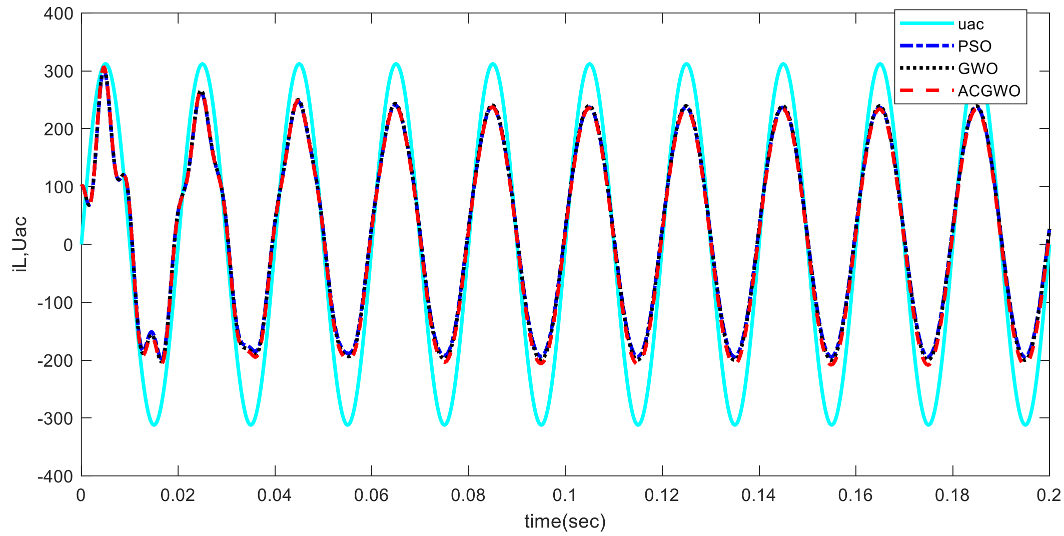

(a)

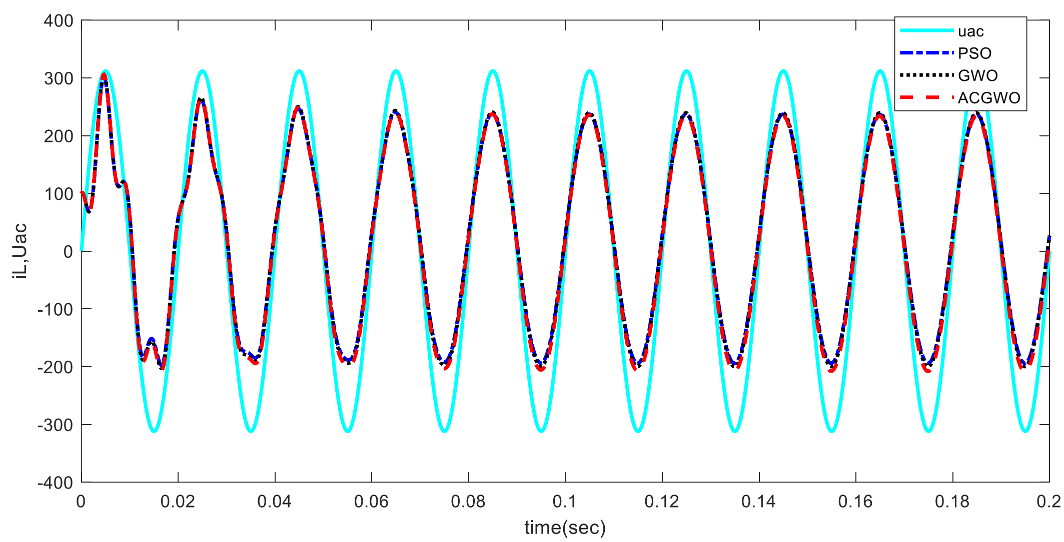

(b)

Fig. 5. The values of i_L and u_{ac} obtained from GWO, PSO and ACGWO a) Main curve, b) magnified curve.

separate sections for phase and frequency synchronization is presented. Since this problem has a large number of local optimums, using intelligent optimization algorithms is necessary. Therefore, in this study, a proposed adaptive chaotic grey wolf optimization (ACGWO) algorithm is used to solve the mentioned problem. To evaluate the performance of the proposed algorithm, simulation results are compared with PSO and GWO. Results show that the proposed algorithm achieves a better cost function in fewer iterations compared to the other two algorithms. In future works, the proposed algorithm can be used for various optimization problems.

REFERENCES

[1] Tong, Y. N., Li, C. L., & Zhou, F. (2016). Synchronization control of single-phase full bridge photovoltaic grid-connected inverter. *Optik*, *127*(4), 1724-1728.

[2] Cotfas, D. T., Deaconu, A. M., & Cotfas, P. A. (2019). Application of successive discretization algorithm for determining photovoltaic cells parameters. *Energy conversion and management*, *196*, 545-556.

[3] Zeb, K., Uddin, W., Khan, M. A., Ali, Z., Ali, M. U., Christofides, N., & Kim, H. J. (2018). A comprehensive review on inverter topologies and control strategies for grid connected photovoltaic system. *Renewable and Sustainable Energy Reviews*, *94*, 1120-1141.

[4] Wang, X., Li, Q., Chen, W., Wang, W., Pu, Y., & Yu, J. (2019). Parallel interaction influence of single-stage photovoltaic grid-connected/hydrogen production multi-inverter system based on modal analysis. *International Journal of Hydrogen Energy*, *44*(11), 5143-5152.

[5] Rodrigo, P. M., Talavera, D. L., Fernández, E. F., Almonacid, F. M., & Pérez-Higueras, P. J. (2019). Optimum capacity of the inverters in concentrator photovoltaic power plants with emphasis on shading impact. *Energy*, *187*, 115964.

[6] Deepamangai, P., & Manoharan, P. S. (2019). Robust controller for grid-connected quasi-admittance source inverter for photovoltaic system. *Electric Power Systems Research*, *175*, 105879.

[7] Lamreoua, A., Benslimane, A., Messaoudi, A., Aziz, A., & El Ouariachi, M. (2018, April). Comparison of the Different Commands Direct and Indirect of a Single-Phase Inverter for Photovoltaic. In *International Conference on Electronic Engineering and Renewable Energy* (pp. 576-586). Springer, Singapore.

[8] Li, S., Liao, Z., Luo, X., Wei, D., Jiang, P., & Jiang, Q. (2018, February). Modeling, numerical simulation, and nonlinear dynamic behavior analysis of PV microgrid-connected inverter with capacitance catastrophe. In *IOP Conference Series: Earth and Environmental Science* (Vol. 121, No. 4, p. 042007). IOP Publishing.

[9] Vaigundamoorthi, M., & Ramesh, R. (2012). Experimental investigation of chaos in input regulated solar PV powered Cuk converter. *International Journal of Computer Applications*, *43*(10), 11-16.

[10] Abusorrah, A., Al-Hindawi, M. M., Al-Turki, Y., Mandal, K., Giaouris, D., Banerjee, S., ... & Papadopoulou, S. (2013). Stability of a boost converter fed from photovoltaic source. *Solar energy*, *98*, 458-471.

[11] Al-Hindawi, M. M., Abusorrah, A., Al-Turki, Y., Giaouris, D., Mandal, K., & Banerjee, S. (2014). Nonlinear dynamics and bifurcation analysis of a boost converter for battery charging in photovoltaic applications. *International*

Journal of Bifurcation and Chaos, *24*(11), 1450142.

[12] Sun, L. X., Li, Y. F., & Wen, Z. G. (2015, November). Fast-scale and slow-scale instabilities of photovoltaic inverter. In *IECON 2015-41st Annual Conference of the IEEE Industrial Electronics Society* (pp. 004597-004602). IEEE.

[13] Chenouard, R., & El-Sehiemy, R. A. (2020). An interval branch and bound global optimization algorithm for parameter estimation of three photovoltaic models. *Energy Conversion and Management*, *205*, 112400.

[14] Chen, Z., Wu, L., Lin, P., Wu, Y., & Cheng, S. (2016). Parameters identification of photovoltaic models using hybrid adaptive Nelder-Mead simplex algorithm based on eagle strategy. *Applied Energy*, *182*, 47-57.

[15] Xu, Y., & Jin, W. (2017). Improvement of parameter identification method for the photovoltaic cell. *Optik*, *132*, 134-141.

[16] Singh, S., & Agrawal, S. (2016). Efficiency maximization and performance evaluation of hybrid dual channel semitransparent photovoltaic thermal module using fuzzyfied genetic algorithm. *Energy conversion and management*, *122*, 449-461.

[17] Zagrouba, M., Sellami, A., Bouaïcha, M., & Ksouri, M. (2010). Identification of PV solar cells and modules parameters using the genetic algorithms: Application to maximum power extraction. *Solar energy*, *84*(5), 860-866.

[18] Soon, J. J., & Low, K. S. (2012). Photovoltaic model identification using particle swarm optimization with inverse barrier constraint. *IEEE Transactions on Power Electronics*, *27*(9), 3975-3983.

[19] Yousri, D., Allam, D., Eteiba, M. B., & Suganthan, P. N. (2019). Static and dynamic photovoltaic models' parameters identification using Chaotic Heterogeneous Comprehensive Learning Particle Swarm Optimizer variants. *Energy conversion and management*, *182*, 546-563.

[20] Zheng, W., & Xiong, X. F. (2013). A model identification method for photovoltaic grid-connected inverters based on the Wiener model. Proc. Chin. Soc. Elect. Eng., 33, 18-26.

[21] Zheng, W., & Xiong, X. F. (2013). System identification for NARX model of photovoltaic grid-connected inverter, Power Syst. Technol. 37, 2440-2445.

[22] Xiong, X. F., Chen, K., Zheng, W., Shen, Z. J., & Nazir, M. S. (2012). Photovoltaic inverter model identification based on least squares method, Power Syst. Prot. Control 40, 52-57.

[23] Adi, F. S., Song, H., & Kim, J. S. (2019). Interlink Converter Controller Design based on System Identification of DC Sub-Grid Model in Hybrid AC/DC Microgrid. *IFAC-Papers Online*, *52*(4), 45-50.

[24] Hart, P. J., Lasseter, R. H., & Jahns, T. M. (2019). Coherency Identification and Aggregation in Grid-Forming Droop-Controlled Inverter Networks.

IEEE Transactions on Industry Applications, *55*(3), 2219-2231.

[25] Khodamoradi, A., Liu, G., Mattavelli, P., Messo, T., & Abedini, H. (2020). PRBS-based loop gain identification and output impedance shaping in DC micro grid power converters. *Mathematics and Computers in Simulation*.

[26] Taheri, S., Kekatos, V., & Cavraro, G. (2019, June). An MILP approach for distribution grid topology identification using inverter probing. In *2019 IEEE Milan PowerTech* (pp. 1-6). IEEE.

[27] Gorbunov, A., Vorobev, P., & Peng, J. C. H. (2020). Identification of Critical Clusters in Inverter-based Micro grids. *arXiv preprint arXiv:2004.00812*.

[28] Ramana, K. V., Majhi, S., & Gogoi, A. K. (2018). Identification of DC–DC buck converter dynamics using relay feedback method with experimental validation. *IET Circuits, Devices & Systems*, *12*(6), 777-784.

[29] Al-Greer, M., Armstrong, M., Ahmeid, M., & Giaouris, D. (2018). Advances on System Identification Techniques for DC–DC Switch Mode Power Converter Applications. *IEEE Transactions on Power Electronics*, *34*(7), 6973-6990.

[30] Xu, J., Armstrong, M., & Al-Greer, M. (2018, June). Parameter Estimation of DC-DC Converters Using Recursive Algorithms with Adjustable Iteration Frequency. In *2018 IEEE 19th Workshop on Control and Modeling for Power Electronics (COMPEL)* (pp. 1-8). IEEE.

[31] Chang, L., Jiang, X., Mao, M., & Zhang, H. (2018, November). Parameter identification of controller for photovoltaic inverter based on LM method. In 2018 IEEE International Power Electronics and Application Conference and Exposition (PEAC) (pp. 1-6). IEEE.

[32] Jiayu, R., Chunlai, L., Yun, T., Xia, Y., & Shengpeng, Y. (2016, November). Modeling of photovoltaic grid connected generation system based on parameter identification method. In *2016 International Conference on Smart City and Systems Engineering (ICSCSE)* (pp. 378-381). IEEE.

[33] Liu, Z., Wu, H., Jin, W., Xu, B., Ji, Y., & Wu, M. (2017). Two-step method for identifying photovoltaic grid-connected inverter controller parameters based on the adaptive differential evolution algorithm. *IET Generation, Transmission & Distribution*, *11*(17), 4282-4290.

[34] Xu, Y., & Jin, W. (2017). A parameter identification model for the Photovoltaic grid-connected inverter. *Optik*, *142*, 23-32.

[35] Mirjalili, S., Mirjalili, S. M., & Lewis, A. (2014). Grey wolf optimizer. *Advances in engineering software*, *69*, 46-61.

[36] Kohli, M., & Arora, S. (2018). Chaotic grey wolf optimization algorithm for constrained optimization problems. *Journal of computational design and engineering*, *5*(4), 458-472.

[37] Teng, Z. J., Lv, J. L., & Guo, L. W. (2019). An improved hybrid grey wolf

optimization algorithm. *Soft computing*, *23*(15), 6617-6631.

[38] Long, W., Jiao, J., Liang, X., & Tang, M. (2018). An exploration-enhanced grey wolf optimizer to solve high-dimensional numerical optimization. *Engineering Applications of Artificial Intelligence*, *68*, 63-80.